WAVE DIFFRACTION ON PLANE BELT WITH DIFFERENT SURFACE IMPEDANCE

T.M. AHMEDOV
Institute of Mathematics and Mechanics of Azerbaijan NAS
AZ-1141, Baku, Azerbaijan, F.Agayev str., 9

The multiple articles [1-3] are dedicated to task solution of wave diffraction on plane belt with ideal boundary conditions (BC). BC of Dirichlet and Neumann types correspond to ideal BC. Such BC appear when it is supposed that belt has ideal electric or magnetic conductivity [1,4]. However, in practice the plane metallic belt has the finite conductivity. In this case the boundary is described by BC of impedance type [4]. From mathematics point of view, BC of third kind corresponds to this boundary [5]. The article [6] is devoted to strong problem solution of wave diffraction on belt with impedance BC. In work [6] the belt surface is described from both sides is described by the one and the same impedance. In the given paper we'll solve the task of E-polarized wave diffraction on the belt the surface of which is described from both sides by the different impedance. By other words the belt is described by two-sided BC. The approach which generalizes the work results for strong solution of this problem is proposed. The proposed method allows constructing the effective numerical algorithms on the base of which the plane dispersion characteristics are calculated.

1. Problem definition

Let's the plane wave falls on plane belt of $2a$ dimension situated in XOZ plane in the center of coordinate system XOY from $y>0$ side.

$$V^i(x,y) = e^{-ik(x\cos\theta + y\sin\theta)} = e^{-ik(x\alpha_0 + y\sqrt{1-\alpha_0^2})} \tag{1}$$

Here $\alpha_0=\cos\theta$, θ is wave incidence angle, $k=\dfrac{2\pi}{\lambda}$ is wave number.

The complete field is presented in the form of sum of incident and scattered fields, i.e.

$$e_z(x,y) = V^i(x,y) + e_z^s(x,y) \tag{2}$$

The complete field should correspond to following conditions:

- everywhere out of belt surface to Helmholtz equation

$$\left(\frac{\partial^2}{\partial x^2} + \frac{\partial^2}{\partial y^2} + k^2\right) e_z(x,y) = 0 \tag{3}$$

- on belt surface to impedance BC of [4] type

$$\frac{\partial e_z}{\partial y} + \frac{ik}{\eta_1} e_z \big|_{y=+0} = 0\,,\ \frac{\partial e_z}{\partial y} - \frac{ik}{\eta_2} e_z \big|_{y=-0} = 0\,,\ |x|<a\,, \tag{4}$$

where η_1, η_2 correspond to impedance on belt surface from $y>0$ and $y<0$ sides correspondingly.

-to Meixner condition on edges [1,7]

-Scattered field $e_z^s(x,y)$ should correspond to condition of Sommerfeld radiation on infinity which has the form [1]

$$\lim_{r\to\infty} \sqrt{r}\left(\frac{\partial}{\partial r} + ik\right) e_z^s(x,y) = 0\,, \tag{5}$$

2. Task solution

Let's write the conception of following type [1,5] for scattered field $e_z^s(x,y)$ on the base of potential theory

$$e_z^s(x,y) = -\frac{i}{4}\int_{-a}^{a} \{f_1(x') + f_2(x')\frac{\partial}{\partial y}\} H_0^{(1)}\left(k\sqrt{(x-x')^2+y^2}\right)dx'\,, \tag{6}$$

here $H_0^{(1)}(x)$ is Hankel function of zero order which corresponds to bivariate Green function of free product. The unknown functions $f_1(x')$ and $f_2(x')$ are potential densities of simple and double layers which correspond to density functions of surface currents and are defined as component jump of complete field on belt surface ($y=\pm 0$), i.e.

$$f_1(x) = \left[\frac{\partial E_z}{\partial y}\right]_-^+ \big|_{y=0}\,,\ f_2(x) = [E_z]_-^+ \big|_{y=0} \quad |x|<a \tag{7}$$

It is seen that perception for scattered field (6) corresponds to Helmholtz equation and condition of radiation on infinity (5).

Let's obey the complete field $e_z(x,y)$ to boundary condition (4) at $y=\pm 0$ for definition of unknown current densities $f_1(x')$ and $f_2(x')$. Taking into consideration (7), we obtain:

$$f_1(x') + ik\left(\frac{E_z^+}{\eta_1} + \frac{E_z^-}{\eta_2}\right) = 0\,,\ |x|<a$$

$$f_2(x') + \frac{1}{ik}\left(\eta_1 \frac{\partial E_z^+}{\partial y} + \eta_2 \frac{\partial E_z^-}{\partial y}\right) = 0\,,\ |x|<a\,. \tag{8}$$

Further we obtain the integral equation (IE) of following type with taking into consideration of (2) and (6) perceptions for definition of $f_1(x)$ and $f_2(x')$ functions:

$$-\frac{1}{k}\frac{2\eta_1\eta_2}{\eta_1+\eta_2}f_1+i\frac{\eta_1-\eta_2}{\eta_1+\eta_2}f_2=2iV^i+\frac{1}{2}\int_{-a}^{a}f_1(x')H_0^{(1)}(k\,|(x-x')\,|)dx', \quad |x|<a \tag{9}$$

$$\begin{aligned}&-i\frac{\eta_1-\eta_2}{\eta_1+\eta_2}f_1+\frac{2k}{\eta_1+\eta_2}f_2=\\&=2i\frac{\partial V^i}{\partial y}|_{y=0}+\frac{1}{2}\lim_{y\to 0}\frac{\partial^2}{\partial y^2}\int_{-a}^{a}f_2(x')H_0^{(1)}(k\sqrt{(x-x')^2+y^2})dx'.\end{aligned} \tag{10}$$

The equations (9) and (10) are Fredholm's IE of second kind with the help of which $f_1(x\ )$ and $f_2(x')$ functions will be defined. Let's rewrite the given IE in images of Fourier $f_1(x\ )$ and $f_2(x')$ functions. With this aim we continue this function by the zero out of $|x|<a$. Then we can write:

$$\left.\begin{aligned}&F_1(\alpha)=\int_{-1}^{1}f_1(a\xi')e^{-i\varepsilon\xi'\alpha}ad\xi'=\int_{-1}^{1}\tilde f_1(\xi')e^{-i\varepsilon\alpha\xi'}d\xi',\ \tilde f_1(\xi')=af_1(a\xi'),\\&F_2(\alpha)=\int_{-1}^{1}f_2(a\xi')e^{-i\varepsilon\xi'\alpha}d\xi'=\int_{-1}^{1}\tilde f_2(\xi')e^{-i\varepsilon\alpha\xi'}d\xi',\ \tilde f_2(\xi')=f_2(a\xi'),\\&\tilde f_1(\xi')=\frac{\varepsilon}{2\pi}\int_{-\infty}^{+\infty}F_1(\alpha)e^{i\varepsilon\alpha\xi'}d\alpha,\ \tilde f_2(\xi')=\frac{\varepsilon}{2\pi}\int_{-\infty}^{+\infty}F_2(\alpha)e^{i\varepsilon\alpha\xi'}d\alpha,\end{aligned}\right\} \tag{11}$$

where $F_1(\alpha)$ and $F_2(\alpha)$ functions are images of Fourier $f_1(x)$ and $f_2(x)$ functions correspondingly and ε, ξ parameters are defined as $\varepsilon=ka$, $x=a\xi$.

Then take into consideration that spectral perception [1,7] takes place for Hankel function $H_0^{(1)}(x)$.

$$H_0^{(1)}(k\sqrt{(x-x')^2+y^2})=\frac{1}{\pi}\int_{-\infty}^{\infty}e^{ik(\alpha(x-x')+|y|\sqrt{1-\alpha^2})}\frac{1}{\sqrt{1-\alpha^2}}d\alpha \tag{12}$$

where that function branch $\sqrt{1-\alpha^2}$ for which $\mathrm{Im}\sqrt{1-\alpha^2}\ge 0$ at $|\alpha|\to\infty$ along real line. This is followed from radiation condition (5).

Substituting (11) and (12) in IE (9) and (10) for Fourier images we obtain IE of following type:

$$Z_1f_1(a\xi)+Z_2f_2(a\xi)=2ie^{-i\varepsilon\xi\alpha_0}+\frac{1}{2\pi}\int_{-\infty}^{\infty}F_1(\alpha)e^{i\varepsilon\xi\alpha}\frac{1}{\sqrt{1-\alpha^2}}d\alpha, \quad |\xi|<1. \tag{13}$$

$$-Z_2f_1(a\xi)+\tilde Z_1f_2(a\xi)=2k\sqrt{1-\alpha_0^2}e^{-i\varepsilon\xi\alpha_0}-\frac{\varepsilon k}{2\pi}\int_{-\infty}^{\infty}F_2(\alpha)e^{i\varepsilon\xi\alpha}\sqrt{1-\alpha^2}d\alpha\ , |\xi|<1. \tag{14}$$

Here Z_1, Z_2, $\tilde Z_1$ parameters which are defined as

$$Z_1=-\frac{1}{k}\frac{2\eta_1\eta_2}{\eta_1+\eta_2},\ Z_2=i\frac{\eta_1-\eta_2}{\eta_1+\eta_2},\ \tilde Z_1=\frac{2k}{\eta_1+\eta_2}. \tag{15}$$

for simplification.

Further multiplying IE (13) and (14) both sides on $e^{i\varepsilon\beta\xi}$ function and integrating on variable ξ in limits [-1,1], we obtain IE of following type:

$$\begin{aligned}&\frac{Z_1}{a}F_1(\beta)+Z_2F_2(\beta)=\\&=4i\frac{\sin\varepsilon(\alpha_0+\beta)}{\varepsilon(\alpha_0+\beta)}+\frac{1}{\pi}\int_{-\infty}^{\infty}F_1(\alpha)\frac{\sin\varepsilon(\alpha-\beta)}{\varepsilon(\alpha-\beta)}\frac{d\alpha}{\sqrt{1-\alpha^2}},\end{aligned} \tag{16}$$

$$\begin{aligned}&-\frac{Z_2}{\varepsilon}F_1(\beta)+\frac{\tilde Z_1}{k}F_2(\beta)=4\sqrt{1-\alpha_0^2}\frac{\sin\varepsilon(\alpha_0+\beta)}{\varepsilon(\alpha_0+\beta)}-\\&-\frac{1}{\pi}\int_{-\infty}^{\infty}F_2(\alpha)\frac{\sin\varepsilon(\alpha-\beta)}{(\alpha-\beta)}\sqrt{1-\alpha^2}d\alpha.\end{aligned} \tag{17}$$

Now let's construct the algorithm of IE solution (16) and (17). As a rule, the desired functions of current density $\tilde f_1(\xi)$ and $\tilde f_2(\xi)$ should correspond to the condition [1,6] in order to scattered field $e_z^s(x,y)$ will correspond to Meixner condition on edges.

$$\tilde f_j(\xi)\underset{\xi\to\pm1}{\approx}(1-\xi^2)^{\nu_j},\ -\frac{1}{2}\le\nu_j\le\frac{1}{2},\ j=1,2;\ \nu_1=-1/2,\ \nu_2=1/2. \tag{18}$$

The value selection of ν_j parameter from interval [-1/2,1/2] depends on physical nature of considered task. In the given case $\tilde{f}_1(\xi)$ function describes the surface current density for which ν_j parameter is equal to $\nu_1=-1/2$. Let's develop $\tilde{f}_j(\xi)$ function in uniformly convergent series on Gegenbauer polynomials of following type for correspondence with condition (18):

$$\tilde{f}_j(\xi)=(1-\xi^2)^{\nu_j}\sum_{n=0}^{\infty} f_n^j C_n^{\nu_j+1/2}(\xi) \quad , \qquad (19)$$

where f_n^j are unknown coefficients, and $C_n^{y_j+1/2}(\xi)$ are Gegenbauer polynomials.

We can obtain the following perception on the base of perception (19) for image of Fourier function $\tilde{f}_j(\xi)$:

$$F_j(\alpha)=\frac{2\pi}{\Gamma(\nu_j+1/2)}\sum_{n=0}^{\infty}(-i)^n f_n^j \beta_n^{\nu_j}\frac{J_{n+\nu_j+1/2}(\varepsilon\alpha)}{(2\varepsilon\alpha)^{\nu_j+1/2}}, \qquad (20)$$

Here $J_n(x)$ is Bessel function $\beta_n^{\nu_j}=\frac{\Gamma(n+2\nu_j+1)}{\Gamma(n+1)}\approx n^{2\nu_j}$ at $n\to\infty$.

Let's substitute the perception for Fourier image (20) in IE (16) and (17) and take into consideration that the following relations [1, 8, 10] take place for values of $\mu_j=\nu_j+1/2\geq 0$ parameter.

$$\frac{1}{\pi}\int_{-\infty}^{\infty}\frac{J_{m+\mu_j}(\varepsilon\beta)}{\beta^{\mu_j}}\frac{\sin\varepsilon(\alpha-\beta)}{\alpha-\beta}d\beta=\frac{J_{m+\mu_j}(\varepsilon\alpha)}{\alpha^{\mu_j}}. \qquad (21)$$

Then we obtain infinite system of linear algebraic equations (ISLAE) of second kind of following type for obtaining unknown f_n^1 and f_n^2:

$$\sum_{n=0}^{\infty} x_n^1[Z_1 d_{mn}^{\mu_1 0}-c_{mn}^{\mu_1}]+Z_2\sum_{n=0}^{\infty} x_n^2 d_{mn}^{\mu_1 1}=4i\gamma_m^{\mu_1},$$
$$m=0,1,2,.. \qquad (22)$$

$$\sum_{n=0}^{\infty} x_n^1\left[-Z_2 d_{mn}^{\mu_2 0}\right]+\sum_{n=0}^{\infty} x_n^2\left[Z_1 d_{mn}^{\mu_2 1}+b_{mn}^{\mu_2 1}\right]=4\sqrt{1-\alpha_0^2}\gamma_m^{\mu_2}. \qquad (23)$$

Here the designations are introduced:

$$x_n^1=\begin{cases} f_0^1, n=0 \\ 2(-i)^n\frac{f_n^1}{n}, n>0\end{cases}, \quad x_n^2=(-i)^n(n+1)f_n^2,$$

$$\gamma_m^{\mu_j}=(-1)m\frac{J_{m+\mu_j}(\varepsilon\alpha)}{\alpha^{\mu_j}}, \qquad (24)$$

$$d_{mn}^{\mu_1 0}=d_{mn}^{00}=\int_{-\infty}^{\infty}\frac{J_n(\varepsilon\beta)J_{m+\mu_1}(\varepsilon\beta)}{\beta^{\mu_1}}d\beta,$$

$$d_{mn}^{\mu_2 1}=d_{mn}^{11}=\int_{-\infty}^{\infty}\frac{J_{n+1}(\varepsilon\beta)J_{m+\mu_2}(\varepsilon\beta)}{\beta^{\mu_2+1}}d\beta,$$

$$c_{mn}^{\mu_1 0}=c_{mn}^{00}=\int_{-\infty}^{\infty}\frac{J_n(\varepsilon\beta)J_{m+\mu_1}(\varepsilon\beta)}{\beta^{\mu_1}\sqrt{1-\beta^2}}d\beta$$

$$b_{mn}^{\mu_2 1}=b_{mn}^{11}=\int_{-\infty}^{\infty}J_{n+1}(\varepsilon\beta)J_{m+\mu_2}(\varepsilon\beta)\frac{\sqrt{1-\beta^2}}{\beta^{\mu_2+1}}d\beta.$$

Note that in all these formulas the parameter $\mu_j=\nu_j+1/2\geq 0$ has the following values $\mu_1=\nu_1+1/2=0$, $\mu_2=\nu_2+1/2=1$.

ISLAE (22) and (23) is related to equation class, which have investigated in detail in work [10]. There it is shown that the reduction method is applied to solution of ISLAE (22) and (23). This means that unknown coefficients f_n^j can be defined with any accuracy. The unknown functions $\tilde{f}_j(\xi)$ characterizing the surface current densities, on which the scattered field $e_z^s(x,y)$ (6) is defined, can be defined on found coefficients f_n^j on the base of formula (19).

3. Integral calculation in matrix elements

The calculation of matrix elements $d_{mn}^{\mu_j 0}, d_{mn}^{\mu_j 1}$, $c_{mn}^{\mu_j 0}$ which are presented by integrals on compositions of Bessel functions, is the main moment at ISLAE solution (22) and (23). The subintegral function becomes quick oscillating one that makes calculation process difficult at increase of ε parameter values. The matrix elements $d_{mn}^{\mu_j 0}$ and $d_{mn}^{\mu_j 1}$ can be calculated in analytic form on the base of table integrals [8]. They have the following form:

$$d_{mn}^{\mu_1 0}=\{1+(-1)^{m+n}\}\frac{1}{\varepsilon}\left(\frac{\varepsilon}{2}\right)^{\mu_1}\frac{\Gamma(\mu_1)\Gamma(\frac{n+m+1}{2})}{\Gamma(\frac{n-m+1}{2})\Gamma(\frac{n+m+2\mu_1+1}{2})\Gamma(\frac{m-n+2\mu_1+1}{2})}, \qquad (25)$$

$$d_{mn}^{\mu_2 1}=\{1+(-1)^{m+n}\}\frac{1}{2}\left(\frac{\varepsilon}{2}\right)^{\mu_2}\frac{\Gamma(\mu_2+1)\Gamma(\frac{n+m+1}{2})}{\Gamma(\frac{n-m+3}{2})\Gamma(\frac{n+m+2\mu_2+3}{2})\Gamma(\frac{m-n+2\mu_2+1}{2})}. \qquad (26)$$

Further the integral calculation in matrix elements $c_{mn}^{\mu_j 0}$ and $b_{mn}^{\mu_j 1}$ can be carried out on the base of algorithms proposed in works [6,12]:

$$c_{mn}^{\mu_1 0}=\{1+(-1)^{n+m}\}I_{mn}^{E}(0,0),$$

$$I_{mn}^{E}(\lambda,\mu)=I_{mn}^{E,1}(\lambda,\mu)-iI_{mn}^{E,2}(\lambda,\mu). \qquad (28)$$

The values $I_{mn}^{E,1}(\lambda,\mu)$ and $I_{mn}^{E,2}(\lambda,\mu)$ are defined in [6,12] and they have the form:

$$I_{mn}^{E,1}(0,0)=\frac{\varepsilon^{m+n}}{2}\sum_{k=0}^{\infty}d_{kmn}^{00}\varepsilon^{2k}\frac{\Gamma(\frac{m+n}{2}+k+\frac{1}{2})}{\Gamma(\frac{m+n}{2}+k+1)} \qquad (29)$$

$$d_{kmn}^{00}=\frac{(-1)^k}{\Gamma(k+1)}\frac{\Gamma(k+\frac{m+n+1}{2})\Gamma(k+\frac{m+n+2}{2})}{\Gamma(k+m+n+1)\Gamma(k+m+1)\Gamma(k+n+1)}$$

Here $\Gamma(\lambda)$ is gamma function.

$$\begin{aligned}I_{mn}^{E,2}(0,0)=[&\sum_{k=0}^{N-1}\frac{1}{2\pi}\Gamma(-k+N)\Gamma(k+\frac{1}{2})\Gamma(k+\frac{1}{2})\Gamma(k+1)\varepsilon^{2k}\}/\\ &/\{\Gamma(k+1)\Gamma(k-N+m+1)\Gamma(k-N+n+1)\Gamma(k+N+1)\}+\\ &+\sum_{k=0}^{\infty}\frac{1}{2\pi}\frac{\Gamma(k+N+\frac{1}{2})}{\Gamma(k+N+1)}d_{kmn}^{00}\varepsilon^{2k+m+n}\{2\ln\varepsilon+2\Psi(k+N+\frac{1}{2})-\\ &-\Psi(k+1)-\Psi(k+m+1)-\Psi(k+n+1)-\Psi(k+m+n+1)\}].\end{aligned} \qquad (30)$$

$$N=\frac{m+n}{2}.$$

The corresponding integrals for index values m=n=0 have the form:

$$I_{00}^{E,2}(0,0)=\sum_{k=0}^{\infty}\frac{1}{2\pi}\frac{\Gamma(k+\frac{1}{2})}{\Gamma(k+1)}d_{k00}^{00}\varepsilon^{2k}\{2\ln\varepsilon+\Psi(k+\frac{1}{2})+\Psi(k+\frac{1}{2})-4\Psi(k+1)\} \qquad (31)$$

The integrals in matrix elements $b_{mn}^{\mu_j 1}$ are calculated on analogous procedure. Let's write the representations for them in the form of rapid-convergent series which have the form:

$$b_{mn}^{\mu_1 1}=b_{mn}^{11}=\{1+(-1)^{n+m}\}I_{mn}^{H}(1,1), \qquad (32)$$

$$I_{mn}^{H}(1,1)=I_{mn}^{H,1}(1,1)+iI_{mn}^{H,2}(1,1), \qquad (33)$$

$$I_{mn}^{H,1}(1,1)=\frac{\varepsilon^{m+n+2}}{4}\sum_{k=0}^{\infty}d_{kmn}^{11}\varepsilon^{2k}\frac{\Gamma(\frac{m+n}{2}+k+\frac{1}{2})}{\Gamma(\frac{m+n}{2}+k+2)}, \qquad (34)$$

$$d_{kmn}^{11}=\frac{(-1)^k}{\Gamma(k+1)}\frac{\Gamma(k+1+\frac{m+n+1}{2})\Gamma(k+2+\frac{m+n}{2})}{\Gamma(k+m+n+3)\Gamma(k+m+2)\Gamma(k+n+2)}, \qquad (35)$$

$$\begin{aligned}I_{mn}^{H,2}(1,1)=[&-\sum_{k=0}^{N-1}\frac{1}{4\pi}\Gamma(-k+N)\Gamma(k+\frac{1}{2})\Gamma(k+\frac{3}{2})\Gamma(k+2)\varepsilon^{2k+2}\}/\\ &/\{\Gamma(k+2)\Gamma(k-N+m+2)\Gamma(k-N+n+2)\Gamma(k+N+3)\}+\\ &+\sum_{k=0}^{\infty}\frac{1}{4\pi}\frac{\Gamma(k+N+\frac{1}{2})}{\Gamma(k+N+2)}d_{kmn}^{11}\varepsilon^{2k+m+n+2}\{2\ln\varepsilon+\Psi(k+N+\frac{1}{2})+\\ &+\Psi(k+\frac{k+m+n+3}{2})+\Psi(k+\frac{k+m+n}{2}+2)-\Psi(k+1)-\Psi(k+m+2)-\\ &-\Psi(k+N+2)-\Psi(k+n+2)-\Psi(k+m+n+3)\}].\end{aligned} \qquad (36)$$

The suggested approach allows forming the high-performance computational algorithms for solution connected with ISLAE (22), (23) on the base of which the calculations of scattering characteristics of plane belt are carried out.

The system of connected ISLAE (22), (23) come undone in one particular case just when the η_1 and η_2 impedance values coincide with each other on low and upper surfaces of belt. Really, parameters Z_1, $\widetilde{Z}_1$, Z_2 take the following values at $\eta_1=\eta_2=\eta$:

$$Z_2=0,\quad Z_1=-\frac{\eta}{k},\quad \widetilde{Z}_1=\frac{k}{\eta}$$

In that case ISLAE (22) and (23) decompose on two independent equation with respect to x_n^1 and x_n^2. These equations coincide with results of work [6].

4. Physical characteristics.

The following parameters: directional diagram (DD), diameters of complete diffusion and backscattering [1,4] are considered in the capacity of physical values characterizing the belt scattering properties. Let's give the definition of these values.

DD characterizes the scattered field behavior in long-distance band which will be written in cylindrical coordinate system in the following form:

$$e_z^s(r,\varphi)\approx A(kr)\phi_E(\varphi),\, kr=k\sqrt{(x^2+y^2)}\to\infty,\quad (37)$$

$$A(kr)=\sqrt{\frac{2}{\pi kr}}e^{i(kr-\pi/4)},\phi_E(\varphi)=\phi_E^1(\varphi)+\phi_E^2(\varphi),\quad (38)$$

$$\phi_E^1(\varphi)=-\frac{i}{4}F_1(\cos\varphi)=-\frac{i\pi}{4}\sum_{n=0}^{\infty}x_n^1J_n(\varepsilon\cos\varphi),\quad (39)$$

$$\phi_E^2(\varphi)=\frac{\varepsilon}{4}\sin\varphi F_2(\cos\varphi)=\frac{\pi}{4}\tan\varphi\sum_{n=0}^{\infty}x_n^2J_{n+1}(\varepsilon\cos\varphi).\quad (40)$$

$\phi_E(\varphi)=\phi_E^1(\varphi)+\phi_E^2(\varphi)$ function describes DD.

The diameters of complete diffusion σ_s^E and backscattering σ^E are defined by the following [1,4]:

$$\frac{\sigma_s^E}{4a}=-\frac{1}{\varepsilon}Re\phi_E(\theta),\quad \frac{\sigma^E}{\lambda}=\frac{2}{\pi}\left|\phi_E(\varphi)\right|^2.\quad (41)$$

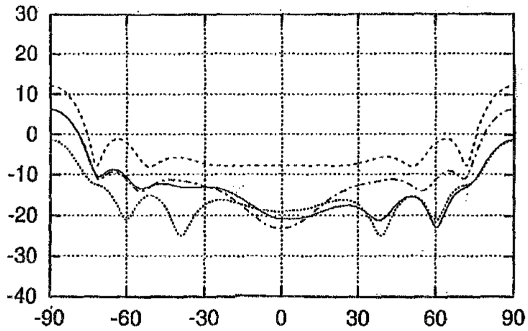

Fig. 1.

The calculation results of diameters of complete diffusion and backscattering on the base of developed efficient computational algorithms are presented on fig.1-4. The dependences of inverse dispersion diameter on angle of incidence for values of frequency parameter $\varepsilon=ka$ (Fig.1 $\varepsilon=5$; Fig.2 $\varepsilon=15$) are shown on fig.1,2. On these figures the dotted curves correspond to impedance values $\eta_1=\eta_2=0$ that corresponds to ideal conducting belt. The curves with dots and dots with line dotted correspond to impedance value $\eta_1=\eta_2=1.5$ and $\eta_1=\eta_2=3.0$ correspondingly. The block curves on these figures correspond to impedance value $\eta_1=3.0$ and $\eta_2=1.5$.

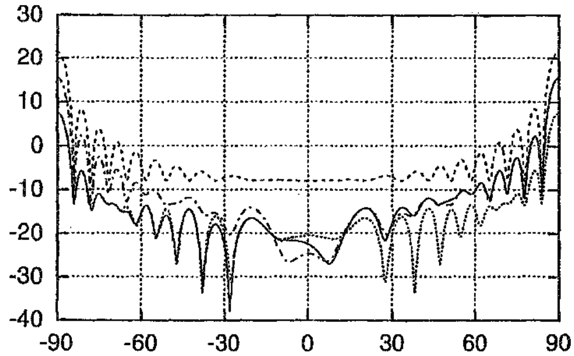

Fig. 2.

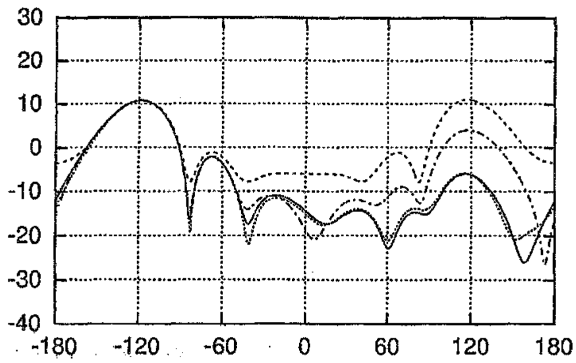

Fig. 3.

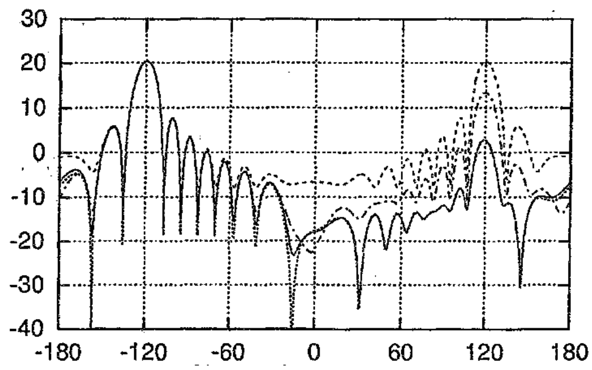

Fig. 4.

DD for values of angle of incidence $\theta=60°$ and $\varepsilon=ka$ (Fig.3 $\varepsilon=5$, Fig.4-$\varepsilon=15$) are presented on the figures 3,4. The order of curve position on impedance values η_1, η_2 is the same as on fig.1,2.

[1] *Kh. Khenl, A. Maye, K. Vestpfal*. Teoriya difraktsii. Moskva: Mir. 1964, -428s**.**

[2] *E.I. Nefedov, A.T. Fialkovskiy.* Asimptoticheskaya teoriya difraktsii elektromagnitnikh voln na konechnikh strukturakh. M.: Nauka. 1972, -247s.

[3] *L.N. Litvinenko, S.L. Prosvirnin*. Spektralnie operatori rasseyaniya v zadachakh difraktsii voln na ploskikh ekranakh. Kiev: Nauk. Dumka, 1984, -240s.

[4] *T.V. Senior and J. Volakis*. Approximate Boundary Conditions in Electromagnetics. The Institution of Electrical Engineers, London, United Kingdom, 1995.

[5] *R.M. Mors, G. Feshbakh*. Metodi teoreticheskoy fiziki. T.1.M. – IL. 1958, -930s.

[6] *T. Ikiz, S. Koshikawa, K. Kobayashi, E.I. Veliev and A.H. Serbest.* Journal of electromagnetic waves and applications. 2001, V.15, n.3, 315-340.

[7] *R. Mittra, S. Li.* Analiticheskie metodi teorii volnovodov. M.-Mir, 1974, -327s.

[8] *A.P. Prudnikov, Yu.A. Brichkov, O.I. Marichev*. Integrali i ryadi (spetsialnie funktsii). M.: Nauka, 1983, -752s.

[9] *I.M. Braver, P.Sh. Fridberg and I.M.Yakovlev.* The behavior of the electromagnetic field near the edge of a resistive half-plane. IEEE Trans. Antennas and Propagat., Vol.AP-36, pp.1760-1768. 1988

[10] *E. Veliev and V.P. Shestopalov*. Sov. Physics dokl., 1988, v.33, n.6, 411-413.

[11] *D.N. Vatson.* Teoriya Besselevikh funktsiy. T.1. M.: IL , 1949, -1000s.

[12] *T.M. Akhmedov*. Fizika, cild 14, №2, s. 75-79.

T.M. Əhmədov

MÜXTƏLIF SƏTHLI IMPEDANSLA MÜSTƏVİ LENT ÜZƏRİNDƏ DALĞALARIN DİFRAKSİYASI

İdeal sərhəd şərtləri ilə müstəvi lentdə dalğaların difraksiya probleminə çoxlu sayda məqalələr [1-3] həsr olunmuşdur. İdeal SŞ-ə Dirixle və Neyman tipli SŞ uyğun gəlir. Belə SŞ-lər ideal elektrik və ya maqnit keçiriciliyinin olduğu güman edildiyi halda yaranır [1-4]. Ancaq praktiki olaraq müstəvi metallik lentlər sonlu keçiriciliyə malikdir. Bu halda sərhədlər SŞ impedans tipinə uyğundur [4]. Riyazi nöqteyi nəzərdən bu sərhədə üçüncü tip SŞ uyğundur. İmpedans SŞ-li lent üzərində difraksiya dalğalarının məsələsinin ciddi həllinə [6] məqalə həsr olunmuşdur. [6] işində lentin səthi hər iki tərəfdən eyni impedansla göstərilmişdir. Bu işdə biz difraksiya məsələsini müstəvi E-polyarizasiyalı dalğa üçün həll edəcəyik. Bu hal impedans SŞ-in xüsusi halıdır. Başqa sözlə lent ikitərəfli SŞ ilə göstərilmişdir. Bu məsələnin ciddi həlli üçün [6] işinin nəticələrini ümumiləşdirən yanaşma təklif olunur.

Т.М. Ахмедов

ДИФРАКЦИЯ ВОЛН НА ПЛОСКОЙ ЛЕНТЕ С РАЗЛИЧНЫМ ПОВЕРХНОСТНЫМ ИМПЕДАНСОМ

Проблеме дифракции волн на плоской ленте с идеальными граничными условиями (ГУ) посвящены многочисленные статьи [1-3]. Идеальным ГУ соответствуют ГУ типа Дирихле или Неймана. Такие ГУ возникают, когда предполагается, что лента имеет идеально электрическую, либо магнитную проводимость [1,4]. Однако, на практике плоская металлическая лента имеет конечную проводимость. В этом случае граница описывается ГУ импедансного типа [4]. С математической точки зрения этой границе соответствует ГУ третьего рода [5]. Строгому решению задачи дифракции волн на ленте с импедансными ГУ посвящена статья [6]. В [6] поверхность ленты с двух сторон описывается одним и тем же импедансом. В данной работе мы построим решение задачи дифракции плоской Е- поляризованной волны на ленте, поверхность которой с двух сторон описывается различным импедансом. Иными словами, лента описывается двусторонними ГУ. Для строгого решения этой задачи предлагается подход, который обобщает результаты работы [6].

Received: 04.03.08